# Theory of Surface Spin Waves in the Heisenberg Ferromagnet

R. E. De Wames and T. Wolfram

*Science Center, North American Rockwell Corporation, 1049 Camino Dos Rios, Thousand Oaks, California 91360*

(Received 27 March 1969)

The eigenvalue matrix for a number of semi-infinite cubic system of spins coupled by nearest neighbors is derived for the Heisenberg ferromagnet. The mathematical formulation used allows solutions for an arbitrary variation in the surface exchange constants. Surface spin-wave modes for the simple cubic structure are calculated for the {100} and {110} surfaces. By allowing the exchange parameters to deviate from the bulk values, the full richness of the surface spin-wave spectra is displayed. Surface spin-wave modes are found to exist above and below the bulk spectrum. The dispersion curves can be truncated, i.e., they exist only over a limited region of $k_{\|}$ space, where $k_{\|}$ is the two-dimensional propagation vector parallel to the crystal surface. The eigenvectors of the surface spin-wave modes are also discussed.

## I. INTRODUCTION

A NUMBER of recent papers have dealt with the problem of calculating surface spin-wave dispersion curves for a ferromagnet.[1-8] The problem is generally approached by selecting out of the total spin Hamiltonian those interactions which dominate in a chosen domain of $k_{\|}$ space, where $k_{\|}$ is the two-dimensional vector of the surface spin wave. The dipole-dominated region, small $k_{\|}$, has been discussed by Eschbach and Damon[6] and more recently by Benson and Mills[7] and by Sparks.[8] The exchange-dominated region has been studied by Wallis et al.,[1] who considered the (100) and (110) "free" surfaces of a simple cubic (sc) ferromagnet. (The term "free" surface is used to characterize a surface for which the exchange parameters are identical to those of the bulk.) They showed that a surface spin-wave branch for a free surface exists only when non-normal exchange bonds are missing at the surface. Thus for a nearest-neighbor exchange model the (100) sc surface does not possess a surface spin-wave branch, while the (110) surface does. A surface spin-wave branch is found for the (100) surface only when second or more distant exchange interactions are included. In contrast to this result, it was shown by Fillipov[2] that a surface spin-wave branch would exist for the (100) surface of a sc in the nearest-neighbor exchange model if the exchange-parameter coupling spins on the surface were different from the bulk exchange. Some errors made by Fillipov have been corrected in a recent paper,[5] where it is shown that if the surface-exchange parameter is larger than that of the bulk, then optical-type surface spin-wave branches lying above the bulk spectrum occur.

The dispersion curve for this new type of mode, defined as the optical branch, may be truncated—i.e., it exists only in a given domain of $k_{\|}$ space.

In the present paper we investigate the properties of surface spin waves for a Heisenberg ferromagnet, using a Green's-function method and keeping only nearest-neighbor interactions. The exchange constants coupling spins parallel and normal to the crystal surface are allowed to differ from their bulk value. The problem reduces to determining the roots of a cubic equation, from which the surface spin-wave energies and eigenvectors are easily obtained.

It is found that when one allows the exchange constants to differ from the bulk values, new physical solutions appear. Consider the model discussed above, in which both the first and second layers of spins are perturbed. Because the exchange constants coupling them differ from the bulk values, there exists a mode having its maximum amplitude on the second layer of spins, in contrast to the mode discussed earlier, in which the amplitude is a maximum on the first layer. It is also found that the dispersion curves may be truncated, and may lie below or above the bulk spectrum depending on the values of the exchange bonds at the surface.

In Sec. II, the theory is presented and a cubic equation whose roots determine the surface eigenmodes is also derived. In Sec. III the eigenvalues and eigenvectors for the {100} and {110} surfaces are discussed for a number of values of the exchange parameters. Conclusions are given in Sec. IV.

## II. THEORY

We consider in this paper only the exchange part of the spin Hamiltonian. Therefore, we have

$$H_s = -\tfrac{1}{2} \sum_{j,\Delta} J(j, j+\Delta) S_j \cdot S_{j+\Delta}, \quad J>0 \qquad (1)$$

where $J$ is the exchange parameter and $S_j$ is the spin angular momentum operator on the $j$th atom. The sum on $\Delta$ is over nearest neighbors only. We define

[1] R. F. Wallis, A. A. Maraduddin, I. P. Ipatova, and A. A. Klockikhin, Solid State Commun. 5, 89 (1967).
[2] B. N. Fillipov, Fiz. Tverd. Tela 9, 1339 (1967) [English transl.: Soviet Phys.—Solid State 9, 1048 (1967)].
[3] D. L. Mills, in *Localized Excitations in Solids*, edited by R. F. Wallis (Plenum Press, Inc., New York, 1968), p. 426.
[4] C. F. Osborne, Phys. Letters 28A, 364 (1968).
[5] R. E. De Wames and T. Wolfram, Phys. Letters (to be published).
[6] J. Eschbach and R. Damon, Phys. Rev. 118, 1208 (1060); J. Phys. Chem. Solids 19, 308 (1961).
[7] H. Benson and D. L. Mills (unpublished).
[8] M. Sparks (unpublished).

the operators

$$L_j = S_{x,j} + i S_{y,j},$$
$$L_j{}^\dagger = S_{x,j} - i S_{y,j}. \qquad (2)$$

Equation (1) can then be written in the form

$$H_s = -\tfrac{1}{2} \sum_{j,\Delta} J(j, j+\Delta)[S_{z,j} S_{z,j+\Delta}$$
$$+ \tfrac{1}{2}(L_j L_{j+\Delta}{}^\dagger + L_j{}^\dagger L_{j+\Delta})]. \qquad (3)$$

The equation of motion for the operator $L_j$ is given by

$$i \frac{d}{dt} L_j = [L_j, H_s], \qquad (4)$$

where $[\cdots]$ means the commutator.

Now, using the commutator relations for the operators $L_j$, $L_j{}^\dagger$, and $S_{z,j}$, and making use of the random-phase approximation (RPA), we obtain for zero temperature

$$\omega L_j(\omega) = S[\sum_\Delta J(j, j+\Delta)]L_j(\omega)$$
$$- S \sum_\Delta J(j, j+\Delta) L_{j+\Delta}(\omega), \qquad (5)$$

where $\langle S_{zj} \rangle = S$ (the total spin of the ion), and where we have introduced the Fourier transform of $L_j(t)$ defined by

$$L_j(t) = \int_{-\infty}^{+\infty} e^{-i\omega t} L_j(\omega) d\omega. \qquad (6)$$

Since the system is invariant under translations parallel to the crystal surface defined by the $zx$ plane, we define the position coordinate of the $j$th atom by $\mathbf{R}_j = (\varrho_j, y_j)$, where $\varrho_j$ is a two-dimensional position vector in the $zx$ plane, and $y_j$ is the position coordinate normal to the surface. We introduce the two-dimensional Fourier transform

$$L_j(\omega) = \frac{1}{(N_s)^{1/2}} \sum_{k_{\text{II}}} \exp(i\mathbf{k}_{\text{II}} \cdot \varrho_j) u_{y_j}(k_{\text{II}}, \omega), \qquad (7)$$

where $N_s$ is the number of surface atoms. After substituting Eq. (7) into Eq. (5) we obtain

$$\omega u_{y_j}(k_{\text{II}}, \omega) = S\{\sum_\Delta J(j, j+\Delta)\} u_{y_j}(k_{\text{II}}, \omega)$$
$$- S \sum_\Delta J(j, j+\Delta) \exp(i k_{\text{II}} \cdot \mathbf{\Delta}_{\text{II}}) u_{y_j+\Delta_\perp}(k_{\text{II}}, \omega), \qquad (8)$$

where $\mathbf{\Delta}_{\text{II}}$ is the component of the position vector of the nearest neighbor parallel to the surface, while $\Delta_\perp$ is the component normal to the surface. In what follows we take the exchange coupling nearest neighbors both on the first layer to be $J_{\text{II}}$, and the exchange coupling nearest neighbors on the first and on the second layer to be $J_\perp$. The exchange between all other nearest

neighbors is taken to be $J$. For this model we can write

$$\omega u_1 = S\{[Z_{\text{II}} J_{\text{II}}(1 - \gamma_{k_{\text{II}}}{}^{(1)}) + Z_\perp J_\perp] u_1$$
$$- Z_\perp J_\perp \gamma_{k_{\text{II}}}{}^{(2)} u_2\},$$
$$\omega u_2 = S\{[Z_{\text{II}} J(1 - \gamma_{k_{\text{II}}}{}^{(1)}) + Z_\perp J_\perp + Z_\perp J] u_2$$
$$- Z_\perp J_\perp \gamma_{k_{\text{II}}}{}^{(2)} u_1 - Z_\perp J \gamma_{k_{\text{II}}}{}^{*(2)} u_3\}, \qquad (9)$$
$$\omega u_n = S\{[Z_{\text{II}} J(1 - \gamma_{k_{\text{II}}}{}^{(1)}) + 2 Z_\perp J] u_n$$
$$- Z_\perp J[\gamma_{k_{\text{II}}}{}^{*(2)} u_{n+1} + \gamma_{k_{\text{II}}}{}^{(2)} u_{n-1}]\}.$$

In the above equation we have labeled the layers by the index $n$ in the $y$ direction. $Z_{\text{II}}$ is the number of nearest neighbors in the layer, and $Z_\perp$ is the number of nearest neighbors in one of the adjacent layers. Also,

$$\gamma_{k_{\text{II}}}{}^{(1)} = \frac{1}{Z_{\text{II}}} \sum_{\mathbf{\Delta}_{\text{II}}{}^{(1)}} \exp[i k_{\text{II}} \cdot \mathbf{\Delta}_{\text{II}}(1)] \qquad (10)$$

and

$$\gamma_{k_{\text{II}}}{}^{(2)} = \frac{1}{2 Z_\perp} \sum_{\mathbf{\Delta}_{\text{II}}{}^{(2)}} \exp[i k_{\text{II}} \cdot \mathbf{\Delta}_{\text{II}}(2)]. \qquad (11)$$

The sum in $\gamma_{k_{\text{II}}}{}^{(1)}$ is over the position vector components of the nearest-neighbor spins in the $xz$ plane for any one layer, while the sum in $\gamma_{k_{\text{II}}}{}^{(2)}$ is over the position vector components in the $xz$ plane coupling neighbors on adjacent layers. For surfaces having $\gamma_{k_{\text{II}}}{}^{(2)}$ real, Eq. (9) can be written in the matrix form

$$(D_N + \Delta D) U_N = 0, \qquad (12)$$

where

$$D_N = \begin{bmatrix} 2\cos\theta & -1 & 0 & \cdots \\ -1 & 2\cos\theta & -1 & \cdots \\ 0 & -1 & 2\cos\theta & \cdots \\ \vdots & \vdots & \vdots & \cdots \end{bmatrix}, \qquad (13)$$

with

$$-(2\cos\theta)\gamma_{k_{\text{II}}}{}^{(2)} Z_\perp = \omega/JS - Z_{\text{II}}(1 - \gamma_{k_{\text{II}}}{}^{(1)}) - 2 Z_\perp, \qquad (14)$$

and where

$$\Delta D = \begin{bmatrix} d_{11} & d_{12} \\ d_{12} & d_{22} \end{bmatrix}, \qquad (15)$$

with

$$d_{11} = [-Z_{\text{II}}(1 - \gamma_{k_{\text{II}}}{}^{(1)})(1 - \epsilon_{\text{II}})$$
$$- Z_\perp(2 - \epsilon_\perp)]/Z_\perp \gamma_{k_{\text{II}}}{}^{(2)},$$
$$d_{12} = (1 - \epsilon_\perp), \quad d_{22} = (\epsilon_\perp - 1)/\gamma_{k_{\text{II}}}{}^{(2)}, \qquad (16)$$
$$\epsilon_{\text{II}} = J_{\text{II}}/J, \qquad \epsilon_\perp = J_\perp/J.$$

We can rewrite Eq. (12) in the form

$$(I_N + G_N \Delta D) U_N = 0, \qquad (17)$$

where $G_N = D_N{}^{-1}$. The elements of $G_N$ can be constructed easily by a variety of mathematical techniques[9] and are given by

$$G_{n,m} = (2i \sin\theta)^{-1}(e^{i(n+m)\theta} - e^{i|n-m|\theta}). \qquad (18)$$

[9] *Selected Papers on Noise and Stochastic Processes,* edited by N. Wax (Dover Publications, Inc., New York, 1954), p. 301.

If the imaginary part of $\theta$ is greater than zero, then $\mathrm{Im}\theta > 0$. The surface eigenvalue equation is obtained by requiring the determinant of Eq. (17) to vanish:

$$|I_N + G_N \Delta D| = 0. \quad (19)$$

Since $\Delta D$ is a $2 \times 2$ matrix, we find

$$1 + G_{11}d_{11} + G_{12}(2d_{12} + d_{11}d_{22} - d_{12}{}^2) + G_{22}d_{22} = 0. \quad (20)$$

Setting $\theta = i\psi$ and $x = e^\psi$ we obtain, according to Eqs. (18) and (20), a cubic in $x$ given by

$$x^3 + x^2(d_{11} + d_{22}) + x(2d_{12} + d_{11}d_{22} - d_{12}{}^2) + d_{22} = 0. \quad (21)$$

The roots of the above cubic which correspond to physical solutions must have $|x| \geqslant 1$, since $\mathrm{Im}\theta > 0$. Equation (21) is valid for any cubic crystal surface. In the following sections we consider two special crystal geometries of the sc ferromagnet and investigate the properties of their surface states.

### III. sc STRUCTURE

#### A. (100) Surface

The crystal structure for the (100) surface is illustrated in Fig. 1 with the coordinate system discussed earlier. The $xz$ plane is taken for all subsequent cases to lie in the surface layer, while the $y$ axis is taken normal to this surface.

We write Eq. (21) in the form

$$x^3 + bx^2 + cx + d = 0. \quad (22)$$

For the (100) surface it is easily shown that

$$\begin{aligned} b &= -(3 - 2\epsilon_\perp) - 4\Lambda_q(1 - \epsilon_{||}), \\ c &= (1 - \epsilon_\perp)[3 + 4\Lambda_q(1 - \epsilon_{||})], \\ d &= \epsilon_\perp - 1. \end{aligned} \quad (23)$$

Also, we see that

$$\cosh\psi = 2\Lambda_q + 1 - \omega_N = \tfrac{1}{2}(x + 1/x), \quad (24)$$

with

$$\begin{aligned} \omega_N &= (\omega/2JS), \quad \Lambda_q = 1 - \gamma_q, \\ \gamma_q &= \tfrac{1}{2}(\cos q_x a + \cos q_z a). \end{aligned} \quad (25)$$

We first consider the case discussed by Fillipov,[2] for which $\epsilon_\perp = 1$.

##### 1. $\epsilon_\perp = 1$, $0 \leqslant \epsilon_{||} \leqslant \infty$

Since for this case $c = d = 0$, Eq. (22) reduces to

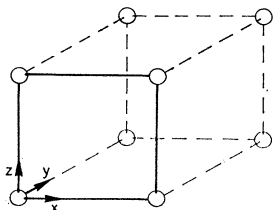$$x = 4\Lambda_q(1 - \epsilon_{||}) + 1. \quad (26)$$



FIG. 1. Sketch of the sc structure and the coordinate system.

Solving Eqs. (24) and (26) simultaneously we obtain

$$\omega_N = 2\Lambda_q[1 + 4\Lambda_q\epsilon_{||}(1 - \epsilon_{||})]/[1 + 4\Lambda_q(1 - \epsilon_{||})]. \quad (27)$$

Equation (26) is identical to Eq. (19) of Ref. 2. As pointed out in an earlier paper,[5] some caution must be used when employing Eq. (27), since it contains energy solutions for $\epsilon_{||} > 1$ which are unphysical in the sense that, according to Eq. (26), they correspond to spin-wave amplitudes which grow with the distance $y$ into the crystal. Since we require $|x| \geqslant 1$, it follows from Eq. (26) that no solutions are allowed for $1 < \epsilon_{||} < 5/4$ for $0 \leqslant \Lambda_q \leqslant 2$. For $0 \leqslant \epsilon_{||} \leqslant 1$, Eq. (26) can always be satisfied with $|x| \geqslant 1$, and the corresponding eigenvalues follow from Eq. (27). For the value $\epsilon_{||} = 1$ (which corresponds to the case discussed by Wallis et al.),[1] Eq. (27) gives the bulk energies, and it is necessary to include second neighbors in order to obtain a
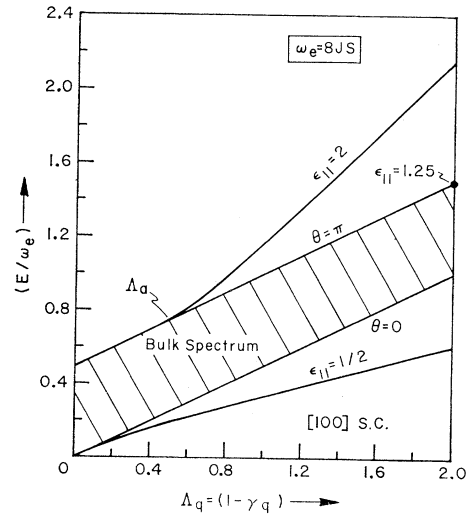


FIG. 2. Dispersion curves for the (100) surface of the sc structure; $\epsilon_\perp = 1$.

surface-state spin-wave branch. In Fig. 2 we illustrate the energy spectrum for two cases, $\epsilon_{||} = 2$ and $\epsilon_{||} = \tfrac{1}{2}$. The shaded area in the figure represents bulk states according to Eq. (24) with $\Psi = i\theta$, $0 \leqslant \theta \leqslant \pi$. Here $\theta = k_y a$, where $k_y$ is the $y$ component of the three-dimensional propagation vector $\mathbf{k}$. The cutoff value $\Lambda_a$ of $\Lambda_q$ is given, according to Eq. (26), by

$$\Lambda_a = 1/2(\epsilon_{||} - 1). \quad (28)$$

The solid dot in the figure corresponds to $\epsilon_{||} = 5/4$, for which $\Lambda_a = 2$. As $\epsilon_{||} \to \infty$, $\Lambda_a \to 0$, and in the limit the optical branch is defined for all values of $\Lambda_q$. An acoustical branch below the bulk spectrum is also shown in Fig. 2 for $\epsilon_{||} = \tfrac{1}{2}$. The word "optical" is introduced for the modes above the bulk spectrum because an investigation of their eigenvectors shows that the spins on adjacent layers are 180° out of phase, in contrast to the acoustical surface branch, where all

spins are in phase. The eigenvectors will be discussed in detail in a later section.

### 2. $\epsilon_{11}=1$, $0<\epsilon_\perp \leqslant \infty$

For this case the cubic equation can be factored, since one of its roots is $x=1$, which gives a bulk solution. The remaining quadratic is

$$x^2-2(1-\epsilon_\perp)x+1-\epsilon_\perp=0. \qquad (29)$$

The two roots are

$$x=(1-\epsilon_\perp)\pm[\epsilon_\perp(\epsilon_\perp-1)]^{1/2}. \qquad (30)$$

We note immediately that for $0<\epsilon_\perp<1$, $x$ is complex and its magnitude is $<1$, so that it does not correspond to a physical solution. In fact, for $0<\epsilon_\perp<\frac{4}{3}$ no admissible solutions exist. For $\epsilon_\perp=\frac{4}{3}$, where $x=-1$, we
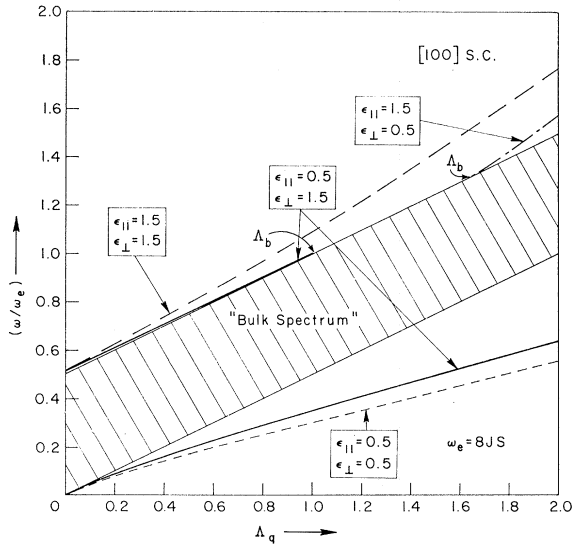


FIG. 3. Dispersion curves for the (100) surface of the sc structure; $\epsilon_\perp<2$.

have a bulk mode corresponding to the case $\theta=\pi$ in Fig. 2. Since for the case $\epsilon_{11}=1$ $x$ is found to be independent of $\Lambda_q$, it follows that the optical surface branch for $\epsilon_\perp>\frac{4}{3}$ lies parallel to and above the bulk branch for $\theta=\pi$.

### 3. $\epsilon_\perp=0$, $0\leqslant\epsilon_{11}\leqslant\infty$

When $\epsilon_\perp=0$, the first layer is completely decoupled from the crystal, and we expect a bulk mode for the case $\epsilon_{11}=1$ having unit-spin amplitude on all layers except the first, and also a mode characteristic of a two-dimensional geometry propagating on the first layer. For this case, since $x=1$ is a solution, the cubic can again be factored, giving
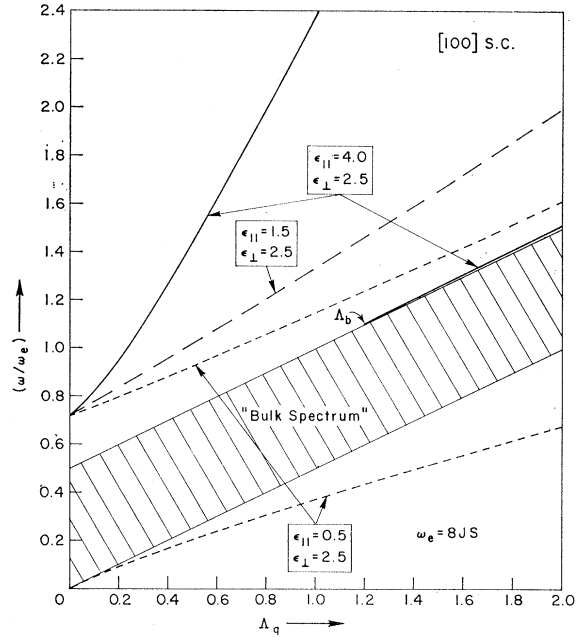
$$x^2-2[1+2\Lambda_q(1-\epsilon_{11})]x+1=0. \qquad (31)$$



FIG. 4. Dispersion curves for the (100) surface of the sc structure; $\epsilon_\perp>2$.

The roots are given by

$$x=1+2\Lambda_q(1-\epsilon_{11})$$
$$\pm\{\Lambda_q(1-\epsilon_{11})[1+\Lambda_q(1-\epsilon_{11})]\}^{1/2}. \qquad (32)$$

We find that for the two-dimensional layer the frequency is given by

$$\omega_N=2\Lambda_q\epsilon_{11}. \qquad (33)$$

### 4. Arbitrary $\epsilon_\perp$ and $\epsilon_{11}$

In this subsection we determine the cutoffs, when they exist, of the optical surface branch for arbitrary value of $\epsilon_\perp$ and $\epsilon_{11}$. These are determined by setting $x=-1$ in the cubic equation (22). We obtain

$$\Lambda_q=\Lambda_b=(6\epsilon_\perp-8)/4(1-\epsilon_{11})(2-\epsilon_\perp). \qquad (34)$$

For $0\leqslant\epsilon_\perp<\frac{4}{3}$ and $0<\epsilon_{11}<1$, there is no optical branch, but only an acoustical branch which approaches the bulk branch $(\theta=0)$ as $\epsilon_{11}$ and $\epsilon_\perp$ increase toward 1 and $\frac{4}{3}$, respectively. Now for $\frac{4}{3}\leqslant\epsilon_\perp<2$ and $0<\epsilon_{11}<1$, we have an acoustical branch and an optical branch. According to Eq. (34) the optical mode cuts off at large values of $\Lambda_q$ as $\epsilon_\perp\rightarrow 2$. For $0<\epsilon_\perp<\frac{4}{3}$ and $1<\epsilon_{11}<\infty$, we have an optical branch which cuts off for small values of $\Lambda_q$ depending on the values of $\epsilon_\perp$ and $\epsilon_{11}$. We have, however, no acoustical branch for this range of parameters. When $\epsilon_\perp>\frac{4}{3}$, the above optical mode becomes allowed for all values of $\Lambda_q$. We illustrate in Fig. 3 the dispersion curves for special values of $\epsilon_{11}$ and $\epsilon_\perp$ in the range just discussed. The next interesting region is for $2<\epsilon_\perp<\infty$. When $0<\epsilon_{11}<1$, according to Eq. (34) there is no cutoff, and, as illustrated in Fig. 4, the optical mode lies above the bulk

curve $\theta=\pi$. The curve below the $\theta=0$ line is the acoustical mode, which exists for all values of $\Lambda_q$. On the other hand, for $1<\epsilon_{11}<\infty$ there exists an optical mode which cuts off for small values of $\Lambda_q$ depending on the values of $\epsilon_\perp$ and $\epsilon_{11}$. For this case we also have another optical branch which lies above the bulk branch $\theta=\pi$. The nature of these modes for the special ranges of parameters is discussed in the next section.

## B. Eigenvectors for (100) Surface of the sc Lattice

From Eq. (17) we have

$$U_N=-G_N\Delta D U_N,\qquad(35)$$

which gives

$$u_l=-[(G_{l1}d_{11}+G_{l2}d_{12})u_1+d_{12}(G_{l1}-G_{l2})u_2].\qquad(36)$$

Let us consider some special cases.

### 1. $\epsilon_\perp=1$

According to Eq. (16), we have

$$u_l=-G_{l1}d_{11}u_1,\qquad(37)$$

since $d_{12}=-d_{22}=0$. Equation (37) can be written as follows:

$$u_l=e^{i(l-1)\theta}u_1,\qquad(38)$$

or

$$u_l=u_1/[1+4\Lambda_q(1-\epsilon_{11})]^{l-1}.\qquad(39)$$

According to Eqs. (2), (6), and (7), at $t=0$ and $\rho_l=0$ the magnitude of the $u_l$'s represents the radius of the precessional circle of the spin, and the sign gives the phase angle of the spin. The index $l$ numbers the layers in the crystal. From Eq. (39), when $0\leqslant\epsilon_{11}\leqslant1$ the phase angle for all layers is zero, but the radius of the precession cone decreases with increasing $l$, i.e., with increasing depth $y$ into the crystal. As discussed previously, in the region $1<\epsilon_{11}<5/4$ there exists no surface branch. However, when $5/4\leqslant\epsilon_{11}\leqslant\infty$ we have a mode (see Fig. 2) above the bulk branch $\theta=\pi$ which cuts off for values of $\Lambda_q<\Lambda_a$. This mode, which is defined as the surface optical branch, has the individual spins rotated 180° between adjacent layers, and their radius of precession decreases with increasing depth $y$ into the crystal.

### 2. $\epsilon_{11}=1$

As discussed in Ref. 1, for this case we always have a bulk mode ($\theta=0$) because of the special geometry of the (100) surface of sc crystals. For this mode all of the $u_l$'s are equal to $u_1$. As discussed in Sec. III, for values such that $0<\epsilon_\perp<\frac{4}{3}$ there is no surface branch. However, when $\frac{4}{3}<\epsilon_\perp<\infty$ there is an optical surface mode above the bulk mode $\theta=\pi$. For this optical surface mode we have $\theta=\pi+i\psi$, with

$$e^\psi=(\epsilon_\perp-1)+[\epsilon_\perp(\epsilon_\perp-1)]^{1/2}.\qquad(40)$$

From Eq. (36) we can solve for $u_2$ in terms of $u_1$. We obtain

$$u_2=\frac{-[-2(1+\cosh\psi)+\epsilon_\perp(1+2\cosh\psi)]u_1}{e^{2\psi}+(1-\epsilon_\perp)(1+2\cosh\psi)}.\qquad(41)$$

For $\epsilon_\perp\gg1$, according to Eqs. (40) and (41), we have

$$u_2\simeq-u_1[1+1/(2\epsilon_\perp)].\qquad(42)$$

Now, inserting Eq. (42) into Eq. (36), we get for $\epsilon_\perp\gg1$

$$u_l=(-1)^{l+1}u_1/(2\epsilon_\perp)^{l-2},\qquad(43)$$

so that in the limit of large values of $\epsilon_\perp$, the amplitudes on the first and second layer are equal. For values of $l>2$ the amplitudes fall rapidly with depth into the crystal.

### 3. $\epsilon_\perp=0$

In this case we have a two-dimensional layer of spins decoupled from the crystal. The root $x=1$ gives $u_1=0$ and unit amplitude for all the other amplitudes. This, of course, is the same mode as discussed previously for $\epsilon_\perp=1$ and $\epsilon_{11}=1$. On the other hand, it can be shown that if $x$ is taken to be the physical root of Eq. (32), then the amplitude on the first layer is $u_1$ while all the others are zero.

## C. (110) Surface

For this case the cubic equation (21) has the form

$$x^3+ex^2+fx+g=0,\qquad(44)$$

with

$$e=-[(3-2\epsilon_\perp)+\Lambda_z(1-\epsilon_{11})]\gamma_x^{-1},$$
$$f=1-\epsilon_\perp^2+[\Lambda_z(1-\epsilon_{11})+(2-\epsilon_\perp)](1-\epsilon_\perp)\gamma_x^{-2},\qquad(45)$$
$$g=(\epsilon_\perp-1)\gamma_x^{-1},$$

where

$$\Lambda_z=1-\gamma_z,$$
$$\gamma_z=\cos(q_za),\qquad(46)$$
$$\gamma_x=\cos(q_xa/\sqrt{2}).$$

The energy is given by

$$\omega_N=\Lambda_z+2-\gamma_x(x+1/x).\qquad(47)$$

We now discuss the solutions of Eq. (47) for various ranges of the parameters.

### 1. $\epsilon_\perp=1,\ 0\leqslant\epsilon_{11}\leqslant\infty$

For this case the cubic equation (44) reduces to

$$\gamma_x x=1+\Lambda_z(1-\epsilon_{11}).\qquad(48)$$

Inserting Eq. (48) into Eq. (47), we obtain

$$\omega_N=\frac{1-\gamma_x^2+\Lambda_z[1+\Lambda_z\epsilon_{11}(1-\epsilon_{11})]}{1+\Lambda_z(1-\epsilon_{11})}.\qquad(49)$$

We note first that when $\gamma_x = 1.0$ (i.e., for a mode propagating in the $z$ direction) Eq. (49) is similar to Eq. (27). For the free surface ($\epsilon_{||} = 1$) there is no surface mode, since in this case $\omega_N = \Lambda_z$, the energy of the bulk mode. For values $0 \leqslant \epsilon_{||} < 1$ the surface branch lies below the bulk. For $1 < \epsilon_{||} < 2$, according to Eq. (48), there exists no solution for real values of $\omega_N$. For $2 < \epsilon_{||} \leqslant \infty$ we have an optical branch which cuts off for small values of $\Lambda_q$. The cutoff value $\Lambda_c$ is

$$\Lambda_c = 2/(\epsilon_{||} - 1). \tag{50}$$

If $\gamma_x \neq 0$, then there exists a surface branch even for the case $\epsilon_{||} = 1.0$. For this case, according to Eq. (49),

$$\omega_N = 1 - \gamma_x^2 + \Lambda_z. \tag{51}$$

For $\theta = 0$ the bulk mode eigenfrequency is

$$\omega_N^{(B)} = 2(1 - \gamma_x) + \Lambda_z. \tag{52}$$

Equation (51) was previously derived in Ref. 1 in order to illustrate the fact that surface modes can exist for nearest-neighbor interactions at a free surface if non-normal bonds are cut in constructing the surface. In Fig. 5 we represent the bulk modes by the shaded portion of the figure. The curve labeled $\epsilon_{\perp} = 1.0$ is a plot of Eq. (51) with $\Lambda_z = 0$. For values of $\Lambda_z \neq 0$ and $\epsilon_{||} = 1.0$, the difference $\omega_N^{(B)} - \omega_N$ is independent of $\Lambda_z$. For $0 \leqslant \epsilon_{||} < 1$, and for values of $\Lambda_z \neq 0$, the surface branch lies below the bulk branch for every value of $\Lambda_x$. This feature is illustrated in Figs. 6 and 7 by the curves labeled $\epsilon_{||} = \frac{1}{2}$ and $\epsilon_{\perp} = 1$. For $1 \leqslant \epsilon_{||} < 2$ we have cutoffs in the dispersion curves. The surface branch touches the bulk at a value of $\Lambda_x$. The surface branch as a function of $\Lambda_x$ is either above the bulk spectrum or below the bulk spectrum, depending on the value of $\Lambda_z$. These cutoffs are obtained from Eq. (48) by requiring $x = \pm 1$.

For $x = +1$,

$$\Lambda_d = \Lambda_z(\epsilon_{||} - 1). \tag{53}$$

According to Eq. (53), when $\epsilon_{||} = 1$ the surface mode and the bulk mode have a common point at $\Lambda_x = 0$. For values of $\epsilon_{||} > 1$, the cutoff value of $\Lambda_x$ approaches 1 as $\Lambda_z$ is increased to its maximum value of 2. The surface branch collapses to a point at $\Lambda_x = 1$, for a given value of $\epsilon_{||}$, when the value of $\Lambda_z$ is $1/(\epsilon_{||} - 1)$. For values of $\Lambda_z > 1/(\epsilon_{||} - 1)$ a new optical branch appears above the top of the bulk spectrum and cutoffs occur on the curve labeled $\theta = \pi$. These cutoffs are obtained by setting $x = -1$ in Eq. (53). This gives

$$\Lambda_x = \Lambda_e = 2 + \Lambda_z(1 - \epsilon_{||}). \tag{54}$$

In Fig. 6 we show the surface branch for $\epsilon_{||} = 2$, $\epsilon_{\perp} = 1.0$, and $\Lambda_z = \frac{1}{2}$. This branch cuts off at $\Lambda_d = \frac{1}{2}$. For this choice of parameters, the branch collapses to a point for $\Lambda_z = 1$ and becomes an optical branch for values of $\Lambda_z > 1$. In Fig. 7 we illustrate the optical branch for $\epsilon_{||} = 2$, $\epsilon_{\perp} = 1.0$, and $\Lambda_z = 2$. According to Eq. (54), the surface branch touches the bulk curve $\theta = \pi$ at $\Lambda_e = 0$.
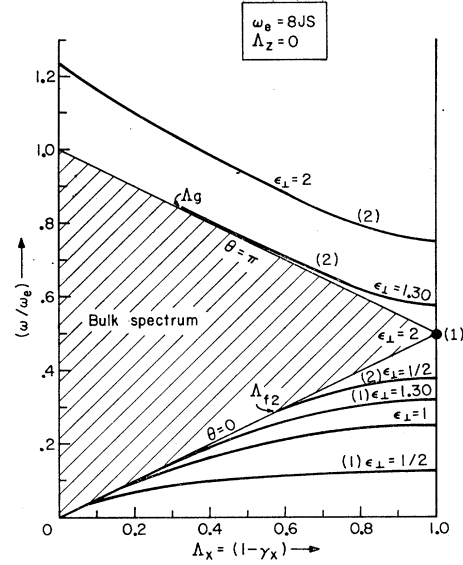


FIG. 5. Dispersion curves for the (110) surface of the sc structure; $\Lambda_z = 0$.

### 2. $\epsilon_{||} = 1, \; 0 < \epsilon_{\perp} \leqslant \infty$

For this case we can take $\Lambda_z = 0$ since the surface modes and the bulk mode have the same functional dependence on $\Lambda_z$. For $0 < \epsilon_{\perp} < 1$ we have two acoustical surface branches. These branches are illustrated in Fig. 5 for $\epsilon_{\perp} = \frac{1}{2}$. The upper branch, labeled (2), cuts off at $\Lambda_x = \Lambda_f$, where

$$\Lambda_f = 1 - (1 - \epsilon_{\perp})(2 - \epsilon_{\perp})/(2 - \epsilon_{\perp}^2), \tag{55}$$

and corresponds to a surface mode which has its maximum amplitude on the second layer of spins. The lower branch, labeled (1), exists for all values of $\Lambda_x$, and has
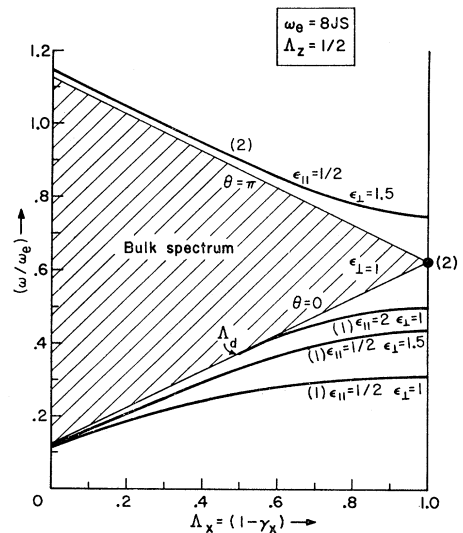


FIG. 6. Dispersion curves for the (110) surface of the sc structure; $\Lambda_z = \frac{1}{2}$.
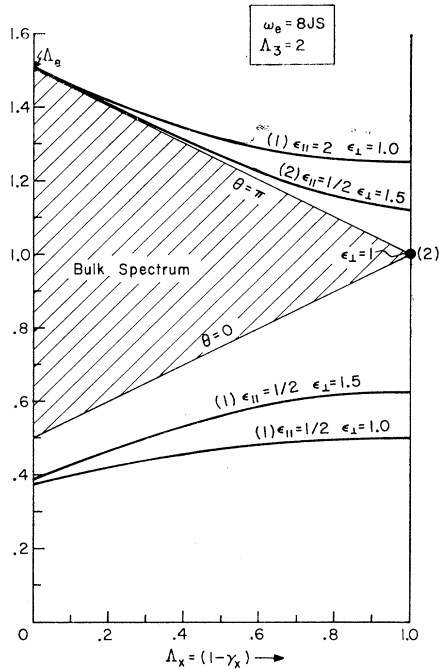
FIG. 7. Dispersion curves for the (110) surface of the sc structure; $\Lambda_z = 2$.

its maximum on the first layer of spins. The presence of two types of modes is physically understandable: In the limit $\epsilon_\perp \to 0$ a surface mode must exist on the second layer, since the first layer is completely decoupled. Hence, as $\epsilon_\perp \to 0$, the surface branch (2) approaches the curve labeled $\epsilon_\perp = 1$. As $\epsilon_\perp \to 0$ the surface branch goes to $\omega/\omega_e \to 0$ for $\Lambda_z$. In the limit of $\epsilon_\perp = 0$ this branch is characterized by $\Lambda_z$ alone and corresponds to energies of a one-dimensional linear chain of spins on the first surface. For this case Eq. (44) can be factored, since one of the roots is $x = 1/\gamma_x$. This root gives a surface mode on the second layer which has zero amplitude on the first layer. The other physical solution is given by

$$\gamma_x x = 1 + (\Lambda_z/2)(1 - \epsilon_{||})$$
$$+ \{[1 + \tfrac{1}{2}\Lambda_z(1 - \epsilon_{||})]^2 - \gamma_x^2\}^{1/2}. \quad (56)$$

The energy of the one-dimensional spin wave may be written, using Eqs. (56) and (47), as

$$\omega_N = \Lambda_z \epsilon_{||}. \quad (57)$$

For $1 \leqslant \epsilon_\perp < \tfrac{4}{3}$ we have two surface branches. One optical-type mode labeled (2) exists above the bulk curve $\theta = \pi$, but cuts off at a small value of $\Lambda_x$, given by

$$\Lambda_x = \Lambda_g = 1 + (1 - \epsilon_\perp)(2 - \epsilon_\perp)/(2 - \epsilon_\perp^2). \quad (58)$$

The other mode is a full acoustical branch lying below the bulk curve $\theta = 0$. In Fig. 5 these two modes are illustrated for $\epsilon_\perp = 1.3$. When $\tfrac{4}{3} \leqslant \epsilon_\perp \leqslant \tfrac{3}{2}$, we have two full surface branches, one lying above the bulk curve $\theta = \pi$, and the other lying below the bulk curve $\theta = 0$. For $\tfrac{3}{2} < \epsilon_\perp < 2$, the acoustical surface branch is truncated

for small values of $\Lambda_x$; the cutoff is given by Eq. (55). The optical surface branch exists for all values of $\Lambda_x$. For $\epsilon_\perp = 2$ the acoustical branch is truncated to a point at $\Lambda_x = 1$, while the optical mode is shifted further from the bulk curve $\theta = \pi$. This is illustrated in Fig. 5 by the curve labeled $\epsilon_\perp = 2$.

For $2 < \epsilon < \infty$ we have two optical modes. One exists for all values of $\Lambda_x$, while the other is truncated for small values of $\Lambda_x$. The cutoff value of $\Lambda_x$ is determined by Eq. (58). We note that $\epsilon_\perp \to \infty$, $\Lambda_g \to 0$. In Figs. 8 and 9 we have plotted Eqs. (55) and (58), respectively. The cutoffs discussed above are given by the portion of the curve which lies in the allowed region of $\Lambda_x$, $0 \leqslant \Lambda_x \leqslant 1$. This region is indicated by the heavy solid line. $\Lambda_f$ gives the cutoffs of the acoustical modes, while $\Lambda_g$ gives the cutoffs of the optical modes.

### 3. Analysis at $\gamma_x = 0$

The two physical roots of Eq. (44), for $\Lambda_z = 0$, are given by

$$x(1) = (2 - \epsilon_\perp)/\gamma_x,$$
$$x(2) = (1 - \epsilon_\perp)/\gamma_x. \quad (59)$$

The energies of these modes follow from Eq. (47):

$$\omega_N(1) = \epsilon_\perp,$$
$$\omega_N(2) = 1 + \epsilon_\perp. \quad (60)$$

The labeling (1) and (2) corresponds to the branches shown in Fig. 5. For $\Lambda_z \neq 0$ and $\epsilon_{||} \neq 1$ the physical roots are given by

$$x(1) = [2 - \epsilon_\perp + \Lambda_z(1 - \epsilon_{||})]/\gamma_x,$$
$$x(2) = (1 - \epsilon_\perp)/\gamma_x. \quad (61)$$

Their energies are

$$\omega_N(1) = \epsilon_\perp + \Lambda_z \epsilon_{||},$$
$$\omega_N(2) = 1 + \epsilon_\perp + \Lambda_z. \quad (62)$$
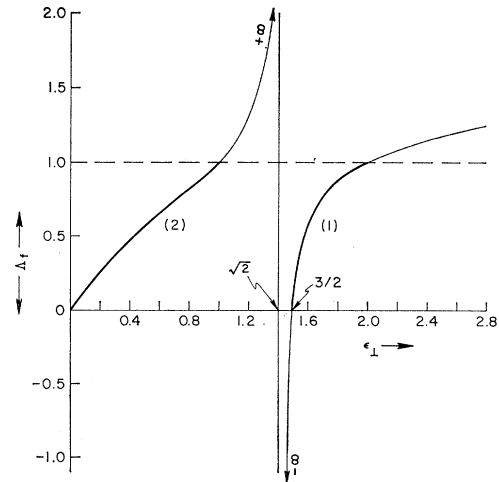


FIG. 8. Cutoff values of $\Lambda_z$ as a function of $\epsilon_\perp$ for surface spin waves below the bulk curve $\theta = 0$.
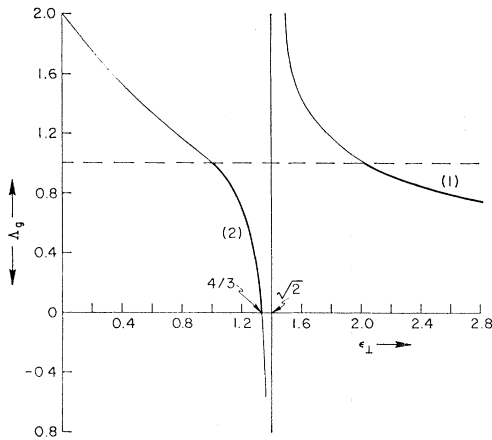
FIG. 9. Cutoff values of $\Lambda_x$ as a function of $\epsilon_\perp$ for surface spin waves above the bulk curve $\theta = \pi$.

According to Eq. (62), the mode on second layer, labeled (2), is not affected by a change in $\epsilon_{||}$ at $\gamma_x = 0$, while the mode at the first layer has a shift proportional to $\epsilon_{||}$ for $\Lambda_z \neq 0$.

#### 4. Arbitrary Values of $\epsilon_\perp$ and $\epsilon_{||}$

In Figs. 6 and 7 we have sketched dispersion curves for a number of values of $\epsilon_\perp$ and $\epsilon_{||}$. The labels (1) and (2) identify the mode for which the amplitude has a maximum on the first and on the second layer of spins, respectively. This identification is, of course, not correct in the limit of $\epsilon_\perp$ and $\epsilon_{||} \rightarrow \infty$, since the amplitudes must then be equal on the two sheets. In the next section we discuss the eigenvectors of these modes for special cases.

### D. Eigenvectors for (110) Surface of the sc Crystal

The eigenvectors for arbitrary values of $\epsilon_{||}$ and $\epsilon_\perp$ are calculable from Eq. (17). Simple analytical forms are obtained for the case $\epsilon_\perp = 1$. It can be shown that

$$u_l = u_1 \gamma_x^{l-1}/[1 + \Lambda_z(1 - \epsilon_{||})]^{l-1}, \qquad (63)$$

since one of the factors of Eq. (44) is

$$x = [1 + \Lambda_z(1 - \epsilon_{||})]\gamma_x^{-1}. \qquad (64)$$

According to Eq. (63), the surface mode for $\gamma_x = 0$ is solely on the first layer of spins. For $\gamma_x \neq 0$ and $1 + \Lambda_z \times (1 - \epsilon_{||}) > 1$, Eq. (63) gives the radius of the precessional circle for the acoustical branch as a function of layer number $l$, counting into the crystal. When $1 + \Lambda_z(1 - \epsilon_{||}) < -1$, the spins are 180° out of phase on adjacent layers, and this mode has been defined as the optical branch.

For the point $\gamma_x = 0$ and $\epsilon_\perp = 1$, one root of the cubic equation (44) depends on the limiting process. This root, according to Eq. (61), is

$$x(2) = (1 - \epsilon_\perp)/\gamma_x. \qquad (65)$$

If $\gamma_x \equiv 0$ and $\epsilon_\perp \rightarrow 0$, then $x(2) \rightarrow \pm\infty$, and we obtain a physical solution. The energy of this state is degenerate with the bulk for $\epsilon_\perp = 1$, but the excitation is

completely localized on the second layer of spins. If $\epsilon_\perp$ is infinitesimally greater than 1, the degeneracy is removed. The existence of this type of mode was missed in Ref. 1 because the surface eigenvectors were assumed to decrease monotonically with increasing depth into the crystal.

## IV. CONCLUSION

By allowing the exchange parameters to deviate from the bulk values, the full richness of surface spin-wave spectra has been displayed. In this paper we have derived for the Heisenberg ferromagnet the eigenvalue matrix for the semi-infinite system of spins coupled by nearest-neighbor exchange. The mathematical formulation used here allows us to obtain solutions for arbitrary values of the surface exchange constants. Surface spin-wave modes for the simple cubic structure are calculated for the (100) and (110) surfaces.

For the (100) surface and only nearest-neighbor interactions, as previously noted in Ref. 1, no surface states exist when $\epsilon_{||} = \epsilon_\perp = 1$ (i.e., for a free surface). However, if these parameters are allowed to vary, surface spin waves below and above the bulk spectrum exist. For a certain range of parameters these surface branches intersect the bulk spectrum. Beyond the point of intersection no surface mode exists for real values of $\omega$. These cutoffs occur because an excitation localized near the surface would decay into a bulk mode of the same frequency and propagation vector. When $\epsilon_\perp \neq 1$, a new surface mode is found to exist, which has its maximum on the second layer of spins. As discussed above, this mode can exist either above or below the bulk spectrum, depending upon the value of $\epsilon_\perp$.

The existence of this mode is physically obvious, since in the limit of $\epsilon_\perp = 0$ the first layer of spins is decoupled from the rest of the crystal, and one must recover for the (100) surface a mode having nonzero amplitude on the first layer with a dispersion curve characteristic of a two-dimensional layer of spins. The other mode which has zero amplitude on the first layer corresponds to the free-surface case.

For the (110) surface and only nearest-neighbor interactions, there is a surface mode characterized by a propagation vector in the $x$ direction (i.e., the [110] direction). As discussed in Ref. 1, the main difference between the (100) and (110) surfaces is that in the latter case non-normal bonds are removed when the surface is constructed. As in the (100) case, two types of surface branches exist for $\epsilon_\perp \neq 1$.

The effect of an external magnetic field simply raises the dispersion curves, but does not affect the damping of the surface spin-wave modes. However, as noted in the Introduction, for small $k_{||}$ the dipolar interactions must be included in the spin Hamiltonian. Some of the physical properties of surfaces not having planar inversion symmetry are discussed in Ref. 10.

---

[10] M. Sparks (unpublished).